Reconfigurable Spatial-Mode-Selective Frequency Conversion in a Three-Mode Fiber

Afshin Shamsshooli[®], Student Member, IEEE, Cheng Guo[®], Graduate Student Member, IEEE, Francesca Parmigiani, Senior Member, IEEE, Xiaoying Li[®], Member, IEEE, and Michael Vasilyev[®], Senior Member, IEEE

Abstract—We present a scheme for spatial-mode-selective frequency conversion in a few-mode fiber and experimentally demonstrate upconversion of arbitrary superpositions of LP_{01} and LP_{11a} signal modes from C-band to the fundamental mode in S-band with all conversion efficiencies within 1 dB range of one another.

Index Terms—Nonlinear fiber optics, nonlinear-optical signal processing, inter-modal four-wave mixing, few-mode fibers, wavelength conversion, quantum communication.

I. Introduction

ODE-DIVISION multiplexing promises increase in Lenannel capacity of both classical and quantum communications [1], [2], hereby bringing attention to multiplexers and demultiplexers of spatial modes. One of desired features of the mode demultiplexer is dynamic reconfigurability of its mode basis. In classical transmission, such reconfiguration could reverse the mode mixing and relax the requirements on electronic processing of the received signals. In quantum key distribution, switching between mutually unbiased mode bases could increase the dimension of the Hilbert space used for encoding. In either case, low loss and low crosstalk of the demultiplexer are important. Not long ago, we have demonstrated such a demultiplexer in a two-mode LiNbO₃ waveguide [3], [4], where, by adjusting the spatial profile of a 1560-nm pump wave, we could selectively upconvert either mode TM₀₀, or mode TM₀₁, or any superposition of these two modes of a 1540-nm signal to TM₀₁ mode at 775 nm, for both classical [3] and single-photon-level [4] signals. More recently, we have proposed a scheme of similar functionality (mode demultiplexing by mode-selective frequency conversion) in

Manuscript received January 15, 2021; revised April 10, 2021; accepted April 19, 2021. Date of publication April 26, 2021; date of current version July 29, 2021. This work was supported in part by the NSF under Grant ECCS-1937860 and Grant ECCS-1842680. (Corresponding author: Afshin Shamsshooli.)

Afshin Shamsshooli, Cheng Guo, and Michael Vasilyev are with the Department of Electrical Engineering, The University of Texas at Arlington, Arlington, TX 76019 USA (e-mail: afshin.shamsshooli@mavs.uta.edu; cheng.guo@mavs.uta.edu; vasilyev@uta.edu).

Francesca Parmigiani is with Microsoft Research, Cambridge CB1 2FB, U.K. (e-mail: francesca.parmigiani@microsoft.com).

Xiaoying Li is with the College of Precision Instruments and Opto-Electronics Engineering, Tianjin University, Tianjin 300072, China (e-mail: xiaoyingli@tju.edu.cn).

Color versions of one or more figures in this letter are available at https://doi.org/10.1109/LPT.2021.3075688.

Digital Object Identifier 10.1109/LPT.2021.3075688

a $\chi^{(3)}$ nonlinear medium, such as a few-mode fiber (FMF), based on a combination of two inter-modal four-wave mixing (IM-FWM) processes [5]. Compared to LiNbO₃ platform, nonlinear FMFs can offer wider design options for mode- and dispersion-engineering and better mode match to the FMFs used in transmission links [6]–[8].

IM-FWM in FMF has recently attracted attention for tunable and broadband wavelength conversion [6], [9]-[12] and correlated photon-pair generation [13]-[15]. IM-FWM in a few-mode fiber has been used for frequency conversion of one out of many wavelength-division multiplexing (WDM) channels on 100-GHz grid with channel selectivity better than 16 dB [10]. IM-FWM-based simultaneous wavelength conversion of many WDM channels encoded with advanced modulation formats has also been demonstrated [11], [12]. In contrast to parametric effects in conventional highly-nonlinear fibers, IM-FWM in FMF uses modal phase-matching and does not require operation in the vicinity of zero-dispersion wavelength, which prevents inter-channel nonlinearities (four-wave mixing, cross-phase modulation) otherwise capable of degrading performance of WDM communication systems. The emergence of nonlinear few-mode fibers with very close values of group velocity dispersion in all modes makes them a promising platform for inter-modal nonlinear-optical signal processing [16].

Realization of mode-selective frequency conversion would enable dynamically reconfigurable mode-division multiplexing. Our preliminary results [5] have shown good crosstalk performance (mode selectivity) for each of the two involved IM-FWM processes individually. In our IPC conference letter [17], we have implemented both of these two processes simultaneously and demonstrated their combined ability to handle any mode superposition in the two-mode (LP₀₁, LP_{11a}) signal space. The present letter is an extended version of [17], providing greater details on the background theory, experimental setup, and measurement procedures, as well as adding graphs demonstrating the mode selectivity/crosstalk for both processes.

II. Theory of $\chi^{(3)}$ -Based Mode-Selective Frequency Conversion

Our scheme of $\chi^{(3)}$ -based mode-selective frequency conversion employs a combination of two IM-FWM processes illustrated in Fig. 1a. We use a graded-index elliptical-core

1041-1135 © 2021 IEEE. Personal use is permitted, but republication/redistribution requires IEEE permission. See https://www.ieee.org/publications/rights/index.html for more information.

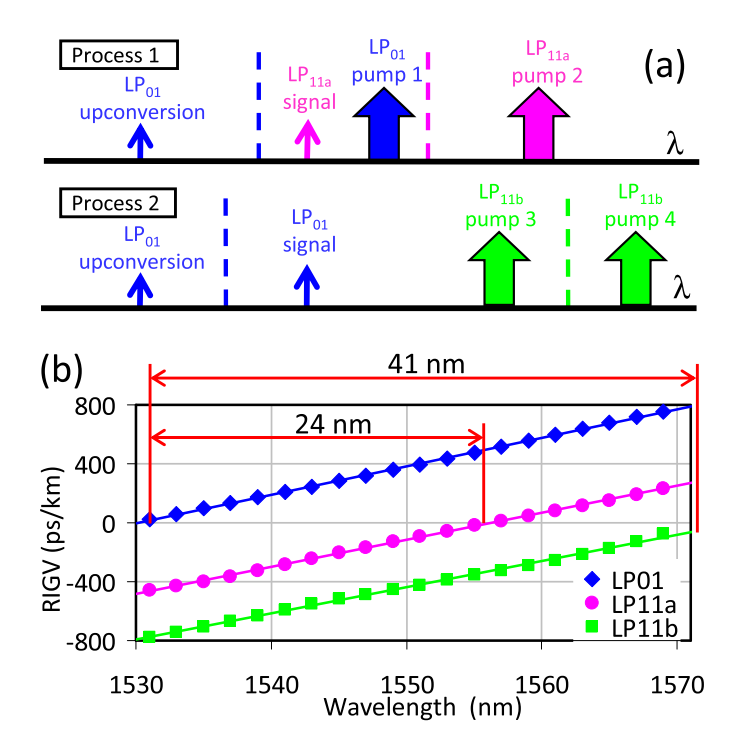


Fig. 1. (a) Two parametric processes, whose combination enables mode-selective frequency upconversion in the TMF. (b) Measured relative inverse group velocity (RIGV) data for the modes of our TMF.

FMF [6] that supports three non-degenerate modes (LP $_{01}$, LP_{11a}, and LP_{11b}), to be referred to as three-mode fiber (TMF) below. Other key fiber properties are as follows [6]: the optical loss is about 0.2 dB/km for all of the modes; the 10% core ellipticity breaks the LP₁₁ mode degeneracy and keeps the distributed crosstalk between any two modes below -27 dB; the calculated effective areas of the LP₀₁ and the LP_{11a,b} modes are 89 μ m² and 125 μ m² at 1550 nm, respectively, resulting in a rather modest value of 0.7/W/km for the inter-modal nonlinear constant and limiting the conversion efficiencies achievable with our available pump power. In IM-FWM process 1, pumps 1 and 2 upconvert LP_{11a} signal to LP₀₁ output mode. In process 2, pumps 3 and 4 upconvert LP₀₁ signal to the same LP₀₁ output mode. With all 4 pumps present, a selected superposition of signal LP₀₁ and LP_{11a} modes is upconverted, whereas the orthogonal mode superposition is left unperturbed. Selection of the mode superposition is done by choosing relative powers of the 2 pairs of pump waves (i.e., relative weights of processes 1 and 2) and pump phase difference $\Delta \varphi = (\varphi_{p1} \varphi_{p2}$) – $(\varphi_{p3} - \varphi_{p4})$. Energy conservation and phase-matching conditions for each process need to be satisfied. Energy conservation laws for wavelength-converted signal (denoted by subscript "WC") in processes 1 and 2 are as follows:

(Process 1)
$$v_{WC} = v_S + v_{P1} - v_{P2}$$
, (1)

(Process 2)
$$\nu_{WC} = \nu_S + \nu_{P3} - \nu_{P4}$$
, (2)

where ν is the optical frequency for each wave, and subscripts "S" and "Pi" denote the signal and i^{th} pump waves, respectively. Note that, if both pumps in either process are identically phase-modulated to suppress stimulated Brillouin scattering, this modulation does not disturb relative phase $\Delta \varphi$ and does not broaden the spectra of the signal and wavelength-converted

beams. IM-FWM selection rules [18] require preservation of the total number of photons in each spatial mode for each process. The phase matching conditions are given by:

(Process 1)
$$\beta^{(01)}(\omega_{WC}) = \beta^{(11a)}(\omega_S) + \beta^{(01)}(\omega_{P1})$$

 $-\beta^{(11a)}(\omega_{P2}),$ (3)
(Process 2) $\beta^{(01)}(\omega_{WC}) = \beta^{(01)}(\omega_S) + \beta^{(11b)}(\omega_{P3})$
 $-\beta^{(11b)}(\omega_{P4}),$ (4)

where β is the propagation constant of each wave, and $\omega = 2\pi \nu$. After Taylor's expansion of $\beta^{(i)}(\omega)$, the phase-matching condition can be reduced to

(Process 1)
$$\beta_1^{(01)} \left(\frac{\omega_{WC} + \omega_{P1}}{2} \right) = \beta_1^{(11a)} \left(\frac{\omega_S + \omega_{P2}}{2} \right),$$
(Process 2)
$$\beta_1^{(01)} \left(\frac{\omega_{WC} + \omega_S}{2} \right) = \beta_1^{(11b)} \left(\frac{\omega_{P3} + \omega_{P4}}{2} \right),$$
(6)

where β_1 denotes the inverse group velocity $1/v_g$.

Phase-matching conditions (5), (6) mean that, for each process, the group velocities at the average frequencies of the two waves present in each spatial mode must be equal [18]. These average frequencies, converted to wavelengths, are shown by the dashed lines in Fig. 1a. Figure 1b shows measured relative inverse group velocities (RIGV) $1/v_g$ of LP₀₁, LP_{11a}, and LP_{11b} modes of our TMF. The LP_{11a} and LP_{11b} curves are approximately parallel to the LP₀₁ curve and are horizontally shifted from it by ~24 nm (Δv_1 = 3 THz) and ~41 nm (Δv_2 = 5.1 THz), respectively. Thus, phase matching is satisfied when the dashed lines in Fig. 1a are separated by 24 nm and 41 nm for processes 1 and 2, respectively, so that we have:

(Process 1)
$$\frac{v_{WC} + v_{P1}}{2} - \frac{v_S + v_{P2}}{2} = \Delta v_1, \quad (7)$$

(Process 2)
$$\frac{v_{WC} + v_S}{2} - \frac{v_{P3} + v_{P4}}{2} = \Delta v_2.$$
 (8)

To satisfy the energy conservation and phase-matching conditions for both processes simultaneously, we have solved the system of Eqs. (1), (2), (7), and (8), which has resulted in the following 4 constraints on the frequencies of the 6 involved waves: $v_{P1} - v_{P2} = v_{P3} - v_{P4} = v_{WC} - v_S = \Delta v_1$ and $v_S = v_{P3} + \Delta v_2 - \Delta v_1$, where v_S (or v_{P3}) and v_{P1} (or v_{P2}) can be chosen arbitrarily. In our experiment, we convert C-band signal at 1542.9 nm to S-band (1519.5 nm), using wavelengths 1554.4, 1578.7, 1560.4, and 1585.1 nm for pumps 1, 2, 3, and 4, respectively.

III. EXPERIMENTAL SETUP

Figure 2 shows the experimental setup. All pumps and the signal are carved into 10-ns-long flat-top pulses with 10-MHz repetition rate by 3 intensity modulators. As shown in Fig. 2a, the pumps are then amplified by telecom-grade C- and L-band erbium-doped fiber amplifiers (EDFAs). As seen in Fig. 2b, pump 2 is converted to LP $_{11a}$ mode by a phase plate PP1, combined with pump 1 in free space by beam splitter BS1, and combined by a free-space beam splitter BS2 with pumps

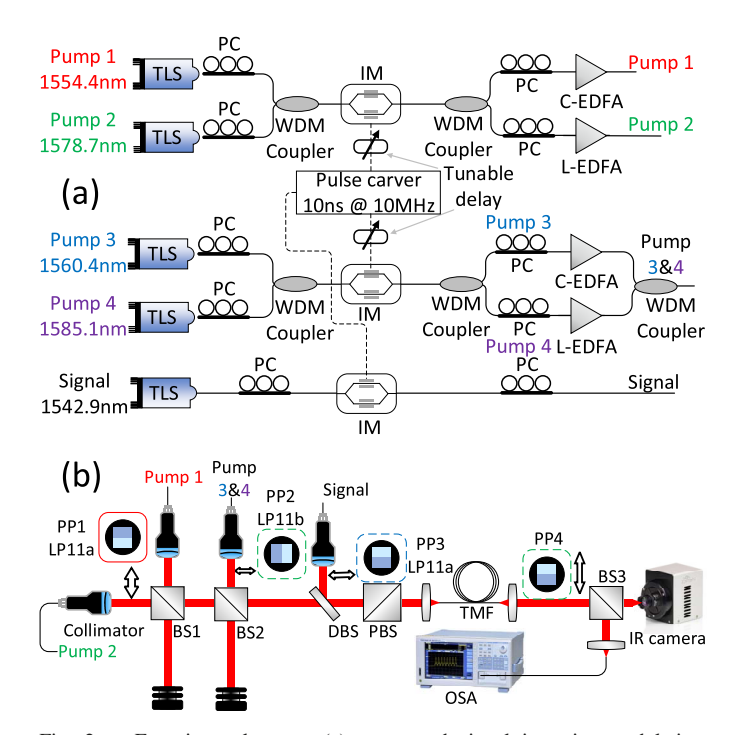


Fig. 2. Experimental setup: (a) pump and signal intensity modulation, synchronization, and amplification; (b) spatial-mode conversion, free-space coupling into the TMF, and output of the IM-FWM experiment.

3 and 4, which have been converted to LP_{11b} mode by a phase plate PP2. All pumps are combined with the signal by a dichroic beam splitter DBS and coupled into the 1-km-long TMF by an objective. The TMF output is split between an infrared camera and a single-mode fiber (SMF) connected to the optical spectrum analyzer (OSA), which in this case measures the LP_{01} "output port" of the TMF. By inserting phase plate PP4 prior to SMF coupling, we can also measure LP_{11a} "output port" of the TMF. We can gradually vary the signal spatial mode from LP_{01} to LP_{11a} by vertically moving the phase plate PP3 (when it is centered on the beam, it generates LP_{11a} mode; when it is far off the center, it leaves the mode in LP_{01} ; in the intermediate positions it generates various two-mode superpositions). To maximize IM-FWM, we co-polarize all three input waves in each process.

IV. RESULTS AND DISCUSSION

Mode selectivity of each individual process is quantified by comparing conversion efficiency (CE) for the "desired" signal mode (LP_{11a} in process 1, LP₀₁ in process 2) to the CE for the "undesirable" signal mode (LP₀₁ in process 1, LP_{11a} in process 2). Inverse of the mode selectivity represents the crosstalk from the undesirable signal mode. Figure 3a shows the spectra illustrating the mode selectivity in process 1, amounting to 20.5 dB. Figure 3b shows 19.8 dB mode selectivity in process 2. In each process, the conversion efficiencies are measured by comparing the power level of the wavelength-converted signal to the power of the original signal. They are found to be -44.3 and -42.7 dB for processes 1 and 2, respectively.

Figure 4 shows the mode-selective frequency conversion spectra with all 4 pumps present (i.e., with both IM-FWM

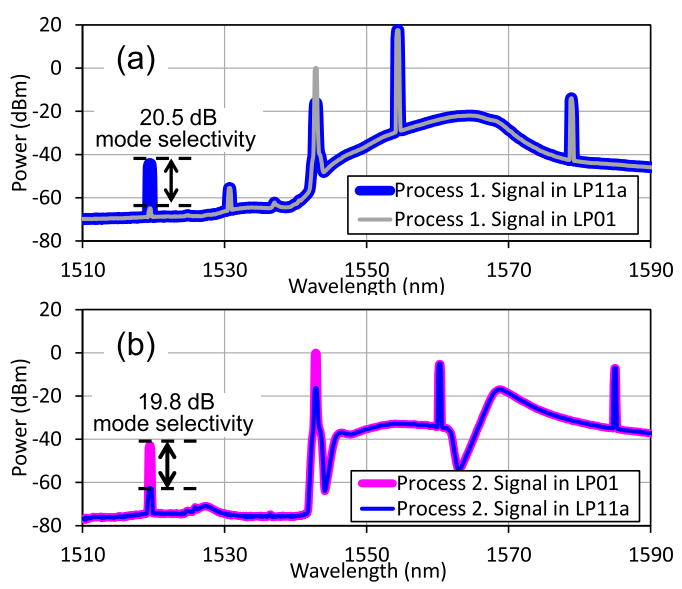


Fig. 3. (a) Optical spectra for process 1 with input signal in either LP_{11a} (thick blue) or LP_{01} (thin gray) mode. (b) Optical spectra for process 2 with input signal in either LP_{11a} (thin blue) or LP_{01} (thick purple) mode. For both graphs, the spectra are measured at the LP_{01} "output port" of the TMF.

processes 1 and 2 taking place simultaneously), where the spatial mode profile of each wave is also shown. Signal spatial mode can be either LP_{01} or LP_{11a} mode, or any superposition of them (the spectra shown in Fig. 4 are obtained with signal in LP_{01} mode). Pump powers have been tuned to nearly equalize the CEs for both processes. Blue spectrum in Fig. 4 is read from LP_{01} output port, and purple spectrum is read from LP_{11a} output port of the TMF. By comparing these two spectra, we have measured the mode purity of the wavelength-converted signal to be better than 14.5 dB. Average powers inside the TMF are 0 dBm for the signal and 17.5, 2.0, 9.5, and 7.5 dBm for pumps 1, 2, 3, and 4, respectively. At these powers, the CEs for processes 1 and 2 are nearly equal (within 0.8 dB of each other).

If we had stable phase $\Delta \varphi = (\varphi_{p1} - \varphi_{p2}) - (\varphi_{p3} - \varphi_{p4})$, we would have been able to select for upconversion a superposition of LP₀₁ and LP_{11a} modes with a specific relative phase. However, such stabilization (based on optical comb) has not been implemented in our setup yet, and our $\Delta \varphi$ fluctuates randomly on 0.1–1 μ s scale. This means that we can observe mode-independent signal upconversion to LP₀₁, as both LP₀₁ and LP_{11a} components of any signal superposition are independently upconverted to LP₀₁ and added incoherently. This is illustrated in Fig. 5, which shows nearly the same CEs (within 1 dB range from one another) measured for various signal superpositions with weight of LP_{11a} component ranging from 0 to 100%.

Our scheme of mode-selective wavelength conversion is highly-selective not only in the spatial domain, but also in the frequency domain, as the phase-matching bandwidth is relatively narrow (0.6 nm). Thus, it can selectively upconvert a single WDM channel from a 100-GHz-spaced WDM grid. By shifting frequencies of all 4 pumps in unison, the frequencies of the signal and converted beams can be easily translated across wide bands of interest. Since the data symbol duration

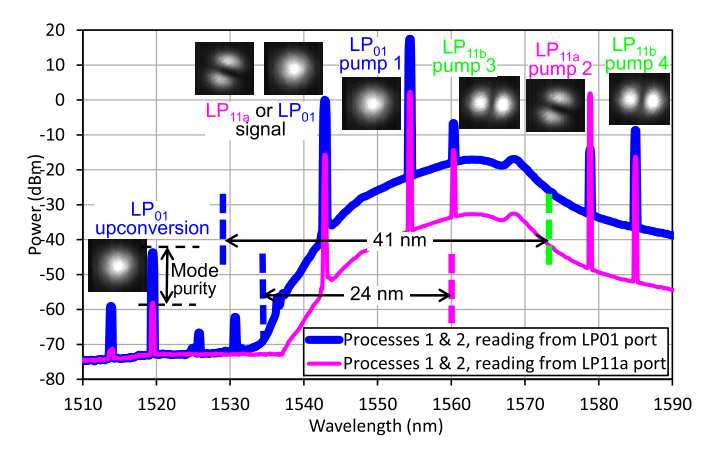


Fig. 4. Spectra of processes 1 and 2 taking place simultaneously and observed through LP_{01} (thick blue) and LP_{11a} (thin purple) output ports. In our experiments, the signal input can be in either LP_{01} or LP_{11a} mode, or any superposition of them. The spectra shown correspond to the input signal in LP_{01} mode.

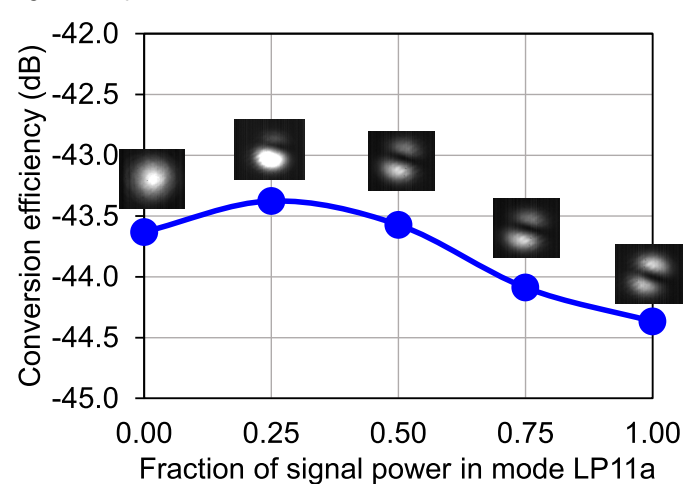


Fig. 5. Conversion efficiencies for various signal mode superpositions.

should be longer than the differential group delay between the original and converted signals, the use of shorter FMF with higher nonlinearity is desirable.

V. SUMMARY

We have simultaneously implemented two inter-modal four-wave-mixing processes necessary for achieving reconfigurable spatial-mode-selective frequency conversion in (LP $_{01}$, LP $_{11a}$) mode space. For these two processes, we have demonstrated conversion efficiencies of -44.3 dB and -42.7 dB and mode selectivities (inverse crosstalk) of 20.5 dB and 19.8 dB, respectively. We have also shown that, in the absence of pump phase stabilization, this scheme can produce mode-independent signal frequency conversion for various superpositions of signal's LP $_{01}$ and LP $_{11a}$ modes. To increase the conversion efficiencies

in the future, one could employ higher-power EDFAs and, possibly, a customized few-mode fiber with a reduced core size and higher nonlinearity.

REFERENCES

- D. J. Richardson, J. M. Fini, and L. E. Nelson, "Space-division multiplexing in optical fibres," *Nature Photon.*, vol. 7, no. 5, pp. 354–362, May 2013.
- [2] Y. Weng, X. He, and Z. Pan, "Space division multiplexing optical communication using few-mode fibers," *Opt. Fiber Technol.*, vol. 36, pp. 155–180, Jul. 2017.
- [3] Y. B. Kwon et al., "Experimental demonstration of spatial-modeselective frequency up-conversion in a multimode χ(2) waveguide," in Proc. CLEO Conf., San Jose, CA, USA, 2016, paper STh3P.4.
- [4] Y. B. Kwon, M. Giribabu, L. Li, C. Langrock, M. Fejer, and M. Vasilyev, "Single-photon-level spatial-mode-selective frequency up-conversion in a multimode χ(2) waveguide," in *Proc. CLEO Conf.*, San Jose, CA, USA, 2017, paper FF2E.1.
- [5] A. Shamsshooli, C. Guo, F. Parmigiani, X. Li, and M. Vasilyev, "Mode-selective frequency conversion in a three-mode fiber," in *Proc. CLEO Conf.*, San Jose, CA, USA, 2020, paper SM3P.3.
- [6] F. Parmigiani et al., "All-optical mode and wavelength converter based on parametric processes in a three-mode fiber," Opt. Exp., vol. 25, no. 26, pp. 33602–33609, Dec. 2017.
- [7] O. F. Anjum *et al.*, "Broadband study of inter-modal Bragg scattering four wave mixing in multi-mode fibres," in *Proc. Eur. Conf. Opt. Commun.*, Rome, Italy, Sep. 2018, pp. 1–3, doi: 10.1109/ECOC. 2018.8535446.
- [8] E. Nazemosadat, A. Lorences-Riesgo, M. Karlsson, and P. A. Andrekson, "Design of highly nonlinear few-mode fiber for C-band optical parametric amplification," *J. Lightw. Technol.*, vol. 35, no. 14, pp. 2810–2817, Jul. 15, 2017.
- [9] O. F. Anjum *et al.*, "Polarization-insensitive four-wave-mixing-based wavelength conversion in few-mode optical fibers," *J. Lightw. Technol.*, vol. 36, no. 17, pp. 3678–3683, Sep. 1, 2018.
- [10] O. F. Anjum et al., "Selective wavelength conversion in a few-mode fiber," Opt. Exp., vol. 27, no. 17, pp. 24072–24081, Aug. 2019.
- [11] G. Rademacher et al., "Experimental investigation of parametric mode and wavelength conversion in a 4.7 km few-mode fiber," in Proc. Eur. Conf. Opt. Commun. (ECOC), Rome, Italy, Sep. 2018, pp. 1–3, doi: 10. 1109/ECOC.2018.8535501.
- [12] G. Rademacher et al., "Wide-band intermodal wavelength conversion in a dispersion engineered highly nonlinear FMF," in Proc. Opt. Fiber Commun. Conf., San Diego, CA, USA, Mar. 2019, pp. 1–3, paper W1C.4.
- [13] D. Cruz-Delgado et al., "Fiber-based photon-pair source capable of hybrid entanglement in frequency and transverse mode, controllably scalable to higher dimensions," Sci. Rep., vol. 6, no. 1, p. 27377, Jun. 2016.
- [14] K. Rottwitt, J. Koefoed, and E. Christensen, "Photon-pair sources based on intermodal four-wave mixing in few-mode fibers," *Fibers*, vol. 6, no. 2, p. 32, May 2018.
- [15] C. Guo, J. Su, Z. Zhang, L. Cui, and X. Li, "Generation of telecomband correlated photon pairs in different spatial modes using few-mode fibers," Opt. Lett., vol. 44, no. 2, pp. 235–238, Jan. 2019.
- [16] G. Rademacher et al., "Investigation of intermodal four-wave mixing for nonlinear signal processing in few-mode fibers," *IEEE Photon. Technol. Lett.*, vol. 30, no. 17, pp. 1527–1530, Sep. 1, 2018.
- [17] A. Shamsshooli, C. Guo, M. Vasilyev, F. Parmigiani, and X. Li, "Reconfigurable mode-selective frequency conversion in a three-mode fiber," in *Proc. IEEE Photon. Conf. (IPC)*, Sep. 2020, pp. 1–2, paper ThF1.2, doi: 10.1109/IPC47351.2020.9252379.
- [18] R.-J. Essiambre et al., "Experimental investigation of inter-modal four-wave mixing in few-mode fibers," *IEEE Photon. Technol. Lett.*, vol. 25, no. 6, pp. 539–542, Mar. 15, 2013.